Pharmaceutical Research, Vol. 24, No. 1, January 2007 (© 2006)
DOI: 10.1007/s11095-006-9140-0

Research Paper

Near Infrared Spectrometry for the Quantification of Human Dermal Absorption of Econazole Nitrate and Estradiol

Joseph P. Medendorp,[1] Kalpana S. Paudel,[1] Robert A. Lodder,[1] and Audra L. Stinchcomb[1,2]

Received May 3, 2006; accepted July 28, 2006; published online November 14, 2006

Purpose. The purpose of this study was to demonstrate the use of near-infrared (NIR) spectrometry for the *in vitro* quantification of econazole nitrate (EN) and estradiol (EST) in human skin.
Methods. NIR spectra were collected from EN and EST powders to verify the presence of NIR chromophores. One percent EN cream, a saturated solution of EN, or 0.25% EST solution was applied to human skin. NIR spectra were collected and one-point net analyte signal (NAS) multivariate calibration was used to predict the drug concentrations. NIR results were validated against known skin concentrations measured by high-pressure liquid chromatography (HPLC) analysis of solvent extracts.
Results. NIR spectroscopy measured dermal absorption from saturated solutions of EN on human skin with an $r^2 = 0.990$, standard error of estimation (SEE) = 2.46%, and a standard error of performance (SEP) = 3.55%, EN cream on skin with an $r^2 = 0.987$, SEE = 2.30%, and SEP = 2.66%, and 0.25% solutions of EST on skin with an $r^2 = 0.987$, SEE = 3.30%, and SEP = 5.66%. Despite low permeation amounts of both drugs through the stratum corneum into human tissue, the NIR signal-to-noise ratio was greater than three, even for the lowest concentrations.
Conclusion. NIR analyses paralleled the results obtained from HPLC, and thus could serve as a viable alternative for measuring the topical bioavailability/bioequivalence of different EN and EST formulations. Because these experiments were conducted in human tissue, this research suggests an all-optical *in vivo* method of measurement for dermal absorption could be developed.

KEY WORDS: chemometrics; dermal drug absorption; econazole; estradiol; net analyte signal; topical bioequivalence.

INTRODUCTION

The drugs used in this study cover two different broad classes of biopharmaceutical goals; a topical drug product category requiring development of a rapid and noninvasive bioavailability/bioequivalence test, and a popular transdermal drug product category requiring development of a rapid and noninvasive test for examining skin drug concentrations after changes in formulation strategy. While it is obvious that topical drug products for local skin treatment need to have a method for biosampling the tissue after product application, it is not as obvious that measuring skin drug concentrations after transdermal treatments is relevant for optimization of drug partitioning and investigation of skin depot effects. The ability to noninvasively sample skin drug concentrations after transdermal product application would allow for easy evaluation of the local effects of skin permeation enhancers, liposomal formulations, gel formulations, microneedle-enhanced delivery, and iontophoresis/sonophoresis-enhanced delivery. The extent and duration of skin depot effects after removal of transdermal patches is a critical part of the evaluation process for these dosage forms. Transdermal studies also require standard systemic plasma sampling for complete bioavailability/bioequivalence determination, but if significant skin drug concentrations do not exist, then there is no need to continue with the time and expense of systemic sampling. The two drugs investigated in this study were econazole nitrate (EN) and estradiol (EST). EN is an antifungal agent that is indicated for the treatment of infections caused by susceptible dermatophyte and candida species, including tinea pedis, tinea cruris, tinea corporis, tinea versicolor and cutaneous candidiasis. A 1% EN topical cream prescription drug product is commercially available from multiple generic manufacturers and Johnson and Johnson (Spectazole® brand name). EST is typically prescribed for hormone replacement therapy in post-menopausal women. In addition to the multiple oral, vaginal, and injectable EST formulations on the market, many brands of transdermal delivery dosage forms are also available. Gels, emulsions, and patches comprise the popular options for non-oral hormone replacement, including Estrogel®, Estrasorb®, Climara-Pro®, Combipatch®, Esclim®, Estraderm®, Menostar™, Vivelle®, Vivelle-Dot® and others.

Current methods for measuring dermal absorption of drugs such as EN and EST include tape stripping (1), punch biopsies, and microdialysis (2). Each of these methods is invasive, causing skin irritation or permanent scarring for the patient or healthy human volunteer. Additionally, quantifi-

[1] Department of Pharmaceutical Sciences, College of Pharmacy, University of Kentucky, 725 Rose Street, Lexington, Kentucky 40536-0082, USA.
[2] To whom correspondence should be addressed. (e-mail: astin2@email.uky.edu)

cation of the drugs sampled during these procedures requires a very time-consuming tissue/fluid extraction step and chromatography-based assay. To illustrate why this is so problematic, consider briefly the phases of the drug development cycle of a topical pharmaceutical product. In preclinical testing, the initial research is conducted and a formulation is developed, followed by phase I, II, and III clinical trials. At each step of the development process, topical bioavailability/bioequivalence must be measured and guaranteed to fall within required therapeutic limits. Preclinical testing alone includes both *in vivo* animal studies and *in vitro* tissue extraction studies, requiring perhaps thousands of tissue samples. Phase I, II, and III clinical trials require 10–80, 100–300, and 1,000–3,000 volunteer test subjects, respectively (3). Before one even takes into account potential studies needed for manufacturing process changes, formulation changes, or generic product development, this process requires a very high number of tissue samples for the development of a single drug product. With inefficient and invasive methods of analysis as the industry standard, an all-optical alternative for measuring dermal absorption is comparatively attractive. An all-optical bioanalytical method is ideally suited as a high-throughput method of analysis for such a demanding drug development process.

As an alternative to processing the tape strips from dermatopharmacokinetic studies with solvent extraction and HPLC analysis, attenuated total reflectance-Fourier transform infrared spectroscopy (ATR-FTIR) has been used to quantify chemicals on the tape strips (4–6). While ATR-FTIR is an improvement over tissue extraction and HPLC, it still requires tape stripping. Because tape stripping is an inefficient method of biosample collection, drug has been demonstrated to continue diffusing faster than the tape strips can be collected (6). This inaccuracy and inconvenience of sample collection demonstrates that there is clearly a place for an all-optical approach for measuring dermal absorption. In our previous study (7), we have demonstrated the utility of NIR spectrometry for the *in vitro* quantification of EN and 4-cyanophenol in hairless guinea pig skin. The purpose of the current study was to investigate the use of NIR spectrometry for the *in vitro* quantification of EN and EST in human skin.

Theory and Instrumentation

NIR spectroscopy can have a tissue penetration depth of many micrometers, millimeters or centimeters depending upon wavelength; making it an analytical method of choice for this research (8,9). Beer's Law states that NIR spectra are the result of a linear combination of the pure component spectra that comprise the sample; therefore, linear multivariate statistics can be used to quantify the analyte of interest even as all other system components change (10). A vector of instrumental responses $\mathbf{r}_k$ can be represented as the sum of two independent signals, the signal from all interferences $\mathbf{r}_k^=$, and the signal from the analyte of interest $\mathbf{r}_k^\perp$, which is orthogonal to the contribution from the interferences (11). This orthogonal portion is termed the net analyte signal (NAS), and is the portion of the signal used for multivariate calibration. Figure 1 illustrates the concept of the NAS. For NAS calibration, only the presence of interferences and their specific spectra must be known *a priori*, not their specific concentrations. A matrix $\mathbf{R}(J\times I)$ without the analyte of interest must be available, where J is the number of wavelengths and I is the number of samples. For the solution exposure experiments, the matrix $\mathbf{R}$ is composed of drug vehicle and a blank tissue spectrum, and for the cream experiments the matrix $\mathbf{R}$ is composed of placebo cream and a blank tissue spectrum. A projection matrix $\mathrm{P}_k^\perp$ can be calculated according to Eq. (1):

$$\mathrm{P}_k^\perp = \left(\mathrm{I} - \mathrm{R}_{-k}\mathrm{R}_{-k}^+\right) \tag{1}$$

where $\mathbf{I}$ is the identity matrix, and the '+' superscript indicates the Moore–Penrose pseudoinverse. Using one-point calibration with spectrum $\mathbf{r}_{cal}$, the NAS vector $\mathbf{r}_{cal}^\perp$ can be calculated with Eq. (2).

$$\mathbf{r}_{cal}^\perp = \mathrm{P}_k^\perp \mathbf{r}_{cal} \tag{2}$$

This vector is then normalized to length one with Eq. (3):

$$\mathbf{r}_k^{NAS} = \frac{\mathbf{r}_{cal}^\perp}{\left\|\mathbf{r}_{cal}^\perp\right\|} \tag{3}$$

The slope of the calibration line can be calculated from (Eq. 4):

$$s = \frac{\left\|\mathbf{r}_{cal}^\perp\right\|}{c_{cal}} \tag{4}$$

where s is the slope and c_{cal} is the analyte concentration of the calibration spectrum. Illustrated in Fig. 2A, the first step of NAS calibration includes using (Eqs. 2–4) to find the NAS direction and determine the length of the NAS vector. As illustrated in Fig. 2B, when the NAS direction and magnitude are known, the unknown spectrum $\mathbf{r}_{un}$ can be projected in the NAS direction with Eq. (5) and its magnitude compared to the calibration magnitude.

$$y_{un}^{NAS} = \mathbf{r}_{un}^T \mathbf{r}_k^{NAS} \tag{5}$$

The ultimate goal of the multivariate calibration is the calculation of the unknown analyte concentration c_{un} which can now be derived with Eq. (6).

$$c_{un} = \frac{1}{s} y_{un}^{NAS} \tag{6}$$

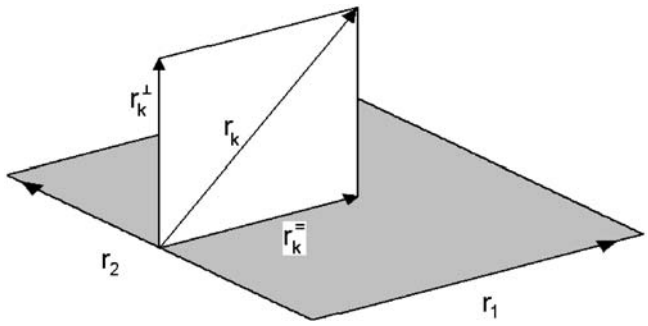

Fig. 1. Figure depicting the NAS for any given analyte. Marked in *gray* is the space spanned by interferences $\mathbf{r}_1$ and $\mathbf{r}_2$. The spectrum of the analyte $\mathbf{r}_k$ is the sum of the NAS vector $\mathbf{r}_k^\perp$ and the interferences.

The NAS approach allows for the calculation of figures of merit from multivariate data sets. In severely overlapping spectra, it has historically been difficult to quantify selectivity, sensitivity, and signal-to-noise (S/N) because of the inability to distinguish between interferences and the analyte of interest (12,13). With the NAS, these quantities can be measured directly. Selectivity is defined as the scalar degree of overlap, α, between the NAS vector and the calibration spectrum according to Eq. (7):

$$\alpha = \frac{\|\mathbf{r}_{cal}^{\perp}\|}{\|\mathbf{r}_{cal}\|} \tag{7}$$

The selectivity is a measure from 0 to 1 indicating how unique the analyte of interest is compared to the interferences. The sensitivity is a measure of the analyte variation in response to a change in concentration. This quantity can be expressed as Eq. (8):

$$\mathbf{s}_k = \mathbf{r}_k^{NAS}/c_k \tag{8}$$

where c_k is the concentration of the k-th analyte. Sensitivity should be the same for each concentration and each NAS vector (14). The S/N ratio can be expressed as Eq. (9):

$$S/N = \frac{c_k\|\mathbf{r}_k^{NAS}\|}{\|\boldsymbol{\varepsilon}\|} \tag{9}$$

where $\boldsymbol{\varepsilon}$ is the random instrumental error.

MATERIALS AND METHODS

Materials

Estradiol (EST), Hanks' balanced salt powder, sodium bicarbonate, ethanol and propylene glycol were purchased from Sigma Chemical (St. Louis, MO). Econazole nitrate (EN), 4-(2-hydroxyethyl)-1-piperazineethanesulfonic acid (HEPES), gentamicin sulfate, trifluroacetic acid (TFA), triethylamine (TEA), potassium phosphate (monobasic and dibasic), sodium hydroxide, polyethylene glycol 400, methanol and acetonitrile (ACN) were obtained from Fisher Scientific (Fair Lawn, NJ). The chemicals were used to make the buffers, donor and receiver solutions for the skin diffusion studies, and for the HPLC mobile phases as described in the respective section below.

Human and Guinea Pig Skin

The diffusion studies were conducted with human skin. Human skin from abdominoplasty surgery was obtained from the National Cancer Institute's Cooperative Human Tissue Network (CHTN). The samples were dermatomed immediately upon arrival to a thickness of approximately 200 μm and frozen at −20°C. On the day of the experiment, the skin was thawed and used for the studies. Skins from three different individuals were used for three different treatments (EST solution, EN solution and EN cream studies).

The hairless guinea pig dorsal skin was blunt dissected from euthanized animals. The procedure was approved by the University of Kentucky IACUC. The skin was dermatomed immediately after dissection to a thickness of approximately 200 μm and frozen at −20°C. On the day of the experiment, the skin was thawed and used for the studies.

Donor Solutions and Creams

Saturated donor solutions of EN were prepared in propylene glycol (20 mg/ml). Donor solutions of EST (0.25%) were prepared in ethanol. One percent EN cream and a corresponding placebo cream were used. Propylene glycol and ethanol were also investigated in order to collect skin spectra from drug vehicle interferences.

In Vitro Diffusion Studies

Teflon MatTek Permeation Devices (MPD, MatTek Corporation, Ashland, MA, USA) were used for the *in vitro* skin diffusion studies with EN and EST solutions. The MPD is essentially a modified form of the Franz diffusion cell that is designed for *in vitro* tissue culture permeation studies. The MPD was the diffusion cell of choice because it requires a

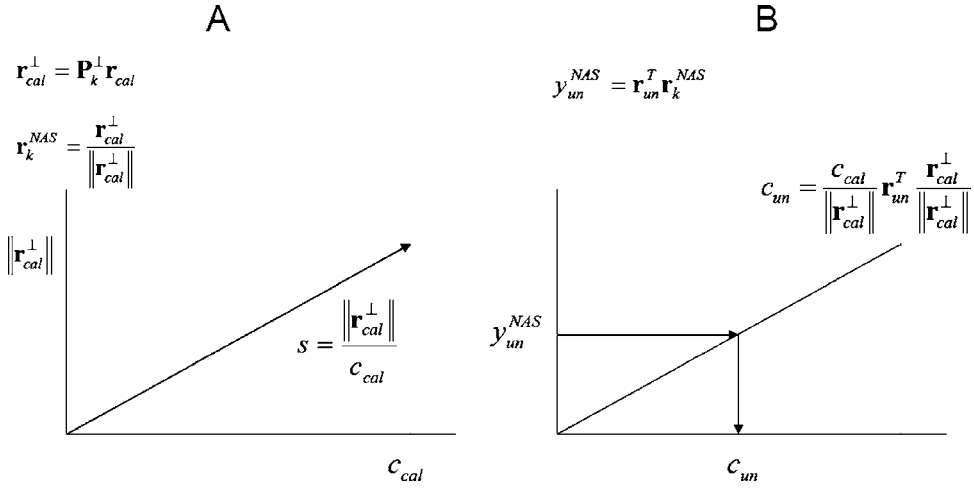

Fig. 2. This figure summarizes the steps for multivariate calibration using the NAS. (A) The first step is to find the NAS direction and calculate the distance of the NAS calibration vector, and (B) the second step is to project the unknown spectrum in the NAS direction and calculate the unknown concentration.

smaller amount of valuable skin (0.196 cm^2), and is a portable and unbreakable Teflon design in contrast to the larger glass Franz cells, which must be used on a large water-circulating/stirring bench. Spacers were used in the wells of the diffusion cells to hold the skin in place. Three MPDs were used for each treatment (donor solution) and exposure time (three per donor solution treatment). The receiver solution was composed of 60% Hanks' pH 7.4 buffer and 40% polyethylene glycol 400 (PEG). The PEG was added to the buffer in order to help solubilize hydrophobic drugs without damaging the skin (2,7).

Skin samples were secured into the MPD and placed in a tightly sealed glass chamber with 10 ml of the receiver solution so that the level of receiver solution remained constant and in contact with the dermis side of the skin. Two hundred microliters of donor solution were added directly onto the stratum corneum from the upper opening of the cell. To prevent the evaporation of the donor solution, cells were capped with vial caps (Waters, Milford, MA, USA). Micro-stirring bars were centered below each diffusion cell and set to stir at a constant rate throughout the experiment.

EN cream studies were conducted in PermeGear modified-Franz flow-through diffusion cells with an area of 1.77 cm^2 and heating blocks maintained at 32°C (PermeGear, Riegelsville, PA), a retriever IV fraction collector (ISCO, Inc., Lincoln, NE), and a Pumppro MPL static pump (Watson Marlow, Wilmington, MA). The FDA has previously recommended 1.77 cm^2 Franz diffusion cells for the *in vitro* testing of topical products. Thus, the present study encompasses both the MPDs, a more practical and portable Teflon-design cell, as well as the standard 1.77 cm^2 diffusion cells. The flow-through cells were only used for the cream studies. The diffusion experiment was initiated by charging the donor compartment with 50 mg of the 1% EN or placebo cream. The cream was applied evenly on the skin with a Teflon rod taking care not to damage the skin. The receiver solution was pumped through the diffusion cells at a flow rate of 1.0 ml/h for 2 h.

At the end of the diffusion experiment, skin samples were removed from the diffusion cells and rinsed with nanopure water three times for 10 s each. In the case of the creams, an alcohol wipe was used to remove excess surface formulation gently. Samples were placed on a paper towel and blotted, and two tape strips (Scotch Book Tape 845) were applied to remove any surface drug. The skin was rinsed one more time with nanopure water, blotted dry with paper towel, and the treated skin area was excised from the center of the skin sample. NIR analysis followed immediately.

Near Infrared Analysis

Drug powders were scanned first to verify the presence of distinct NIR chromophores for EN and EST. A uniform layer of pure drug approximately 1 mm thick was loaded on a one-well depression microscope slide (Gold Seal Products, Portsmouth, NH). NIR spectra from 1,100–2,500 nm were collected in steps of 2 nm with a scanning monochromator system described earlier (15) interfaced to a computer (OptiPlex GXM 5166, Dell, Round Rock, TX, USA) running SESAME 3.1 (Bran + Luebbe, Norderstedt, Germany). To maximize light scatter, microscope slides and samples were placed on top of a 135-degree conical reflecting cup, designed such that when a sample is placed along the axis of radial symmetry of the cone, specular reflection at the detector is minimized while diffuse reflectance is maximized (16). All data were exported to Matlab 7.0.1 (The Mathworks Company, Natick, MA) for processing and analysis. Powder samples and solutions were scanned six times each, rotating them 120 degrees between each scan. Tissue samples were scanned three times from the epidermal side, and three times from the dermal side.

Chemometric Analysis

All chemometric algorithms were written by the authors. NAS calibration requires a matrix of spectra without the analyte such that the region of space spanned by the interferences is included in the calibration model. For quantification of drug absorbed from solutions of EST and EN applied to the tissue, the matrix consisted of a pure component spectrum from drug vehicle (ethanol or propylene glycol) and a blank tissue spectrum exposed to drug vehicle alone. For quantification of EN cream, the matrix consisted of a placebo cream spectrum and a blank tissue spectrum exposed to placebo. With this approach, it was not necessary to identify the regions of the spectrum where the target drug could be quantified. NAS calibration automatically finds the regions of the spectrum orthogonal to the space spanned by the interferences, thus canceling out their effects on the net analyte signal. Figures of merit, such as sensitivity, selectivity, S/N ratio, limit of detection, bias, and precision were also calculated directly from the NAS.

Skin Extraction and HPLC Analysis

Immediately following NIR analysis, the tissue was weighed. The sample was then minced with a scalpel and placed in a vial with 1 or 2 ml of ACN for solution and cream studies, respectively. This vial was sonicated for 10 min and shaken for 15 h at room temperature to extract the drug from the tissue into the ACN. The tissue extract was then analyzed for drug concentration by HPLC analysis, and expressed as μg of drug per wet g of tissue weight. Insoluble material was centrifuged to the bottom of the extract vial, and clear extract samples were placed in HPLC vials. This extraction method provided 90–95% recovery of estradiol and 90–100% recovery of econazole nitrate from injection spiked tissue samples.

The high-pressure liquid chromatography (HPLC) assay was done with a Perkin-Elmer Series 200 Autosampler, Pump, Column Oven (room temperature setting), and a 785A UV/VIS Detector with Turbochrom Professional Version 4.1 Software. A Brownlee® C18 RP Spheri-5 μm column (220×4.6 mm) with a C18 RP 7 μm guard column (15×3.2 mm) was used with the UV/VIS Detector set at a wavelength of 215 nm for EN and 205 nm for EST. The mobile phase used for EN was 70:30 ACN:0.1% TFA adjusted with TEA to a pH of 3.0. The mobile phase used for EST was 45:55 ACN:methanol and distilled water (5 and 50%, respectively). The flow rate of the mobile phase was at 1.0 ml/min for EN and EST. Standards were analyzed with each set of diffusion samples and exhibited excellent linearity over the concentration range employed. The retention times

for EN and EST were 10.02 ± 0.05 min and 10.37 ± 0.03 min, respectively. The sensitivities of the assays for EN and EST were 25 ng/ml and 50 ng/ml, respectively.

RESULTS

To test whether or not there were appreciable differences between the NIR ability to measure drug absorption from the dermal side and the epidermal side, scans were collected from each side and analyzed separately. Using NAS calibration, NIR spectrometry measured an applied dose of 200 µl of saturated EN in propylene glycol on human skin with an $r^2 = 0.988$, a standard error of estimate over the concentration range (SEE) of 2.46%, a standard error of performance over the concentration range (SEP) of 2.86% from the epidermal side, and an $r^2 = 0.996$, SEE = 1.98%, SEP = 2.12% from the dermal side. (See Fig. 3 for the calibration results.) Figure 4 illustrates that NIR spectrometry measured different concentrations of EST in ethanol using NAS calibration with an $r^2 = 0.988$, SEE = 3.46%, SEP = 4.01%. Figure 5 illustrates that NIR measured an applied dose of EST in ethanol on human tissue with an $r^2 = 0.987$, SEE = 3.30%, SEP = 5.66% from the epidermal side, and an $r^2 = 0.967$, SEE = 5.53%, SEP = 6.83% from the dermal side. NIR measured an applied dose of 50 mg of either placebo cream or 1% EN cream with an $r^2 = 0.987$, SEE=2.30%, SEP = 2.66% from the epidermal side, and an $r^2 = 0.987$, SEE=2.53%, SEP=2.83% from the dermal side (data not shown). The drug absorption was extremely high for one tissue sample, however, and these statistics were calculated with the inclusion of a high-end outlier point. This outlier was most likely due to an insufficient surface formulation wash-step in this particular sample; however, it was encouraging to note that both assay methods consistently detected this procedural artifact. Figure 6 illustrates the same scenario with the high-end outlier excluded from the model. In this case, NIR resulted in a calibration r^2=0.981, SEE=5.67%, SEP=6.07% from the dermal side and an r^2=0.980, SEE=5.93%, SEP=6.71% from the epidermal side.

The sensitivity ($\mathbf{s}_k$), selectivity (α), and S/N ratios were calculated according to Eqs. 7–9, respectively. For solutions of EST on human skin, $\mathbf{s}_k$=0.0455, α=0.143, and the S/N = 29.54. For saturated solutions of EN on human skin, $\mathbf{s}_k = 0.0104$, $\alpha = 0.0205$, and the S/N = 10.04, and for EN cream, $\mathbf{s}_k = 0.052$, $\alpha = 0.0778$, and the S/N = 7.763. Selectivity is a unitless quantity, and sensitivity is given in units of signal/concentration. Bias was calculated as the mean of the difference between replicate measurements of each concentration and the reported HPLC true concentration, and precision was calculated by the standard deviation of the difference between replicate measurements at each concentration and the reported HPLC true concentration. Because bias and precision values were calculated for each concentration, the final reported values are the means calculated from the data set in its entirety. For EST on human skin, bias = −16.37 and precision = 1.149. For saturated solutions of EN on human skin, bias = 0.4706, and precision = 3.171, and for EN creams on human skin, bias = 16.03, and precision = 1.357. Both bias and precision are given in units of µg/g.

DISCUSSION

Some multivariate calibration models offer the capability of wavelength and feature selection, such as principal component regression (17), interval partial least squares (18), and uninformative variable elimination (19). These chemometric models require the construction of a large database of calibration samples, to ensure that all sample spectral variations are included in the calibration model. Then, the calibration model is validated by using it to predict the analytical results of a new set of samples through their spectra. This prediction is compared to the results from a reference

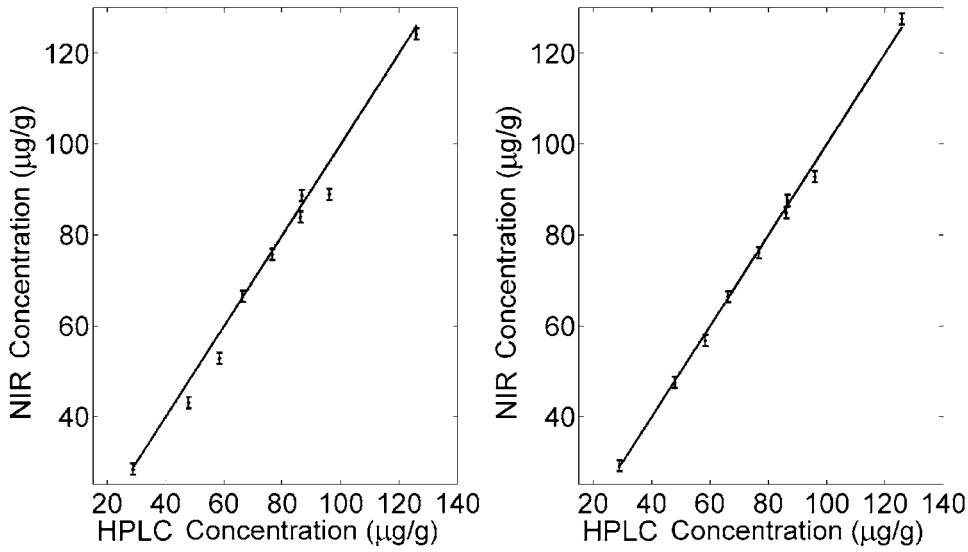

Fig. 3. NIR calibration line from human skin treated with 200 µl of saturated econazole nitrate in propylene glycol, (*left*) epidermis calibration, $r^2 = 0.988$, SEE = 2.46%, SEP = 2.86%, (*right*) dermis calibration, $r^2 = 0.996$, SEE = 1.98%, SEP = 2.12%. The *diagonal line* illustrates the perfect correlation between HPLC and NIR, HPLC concentrations are shown on the *x-axis*, and the *error bars* are the means and standard errors of the NIR measurements.

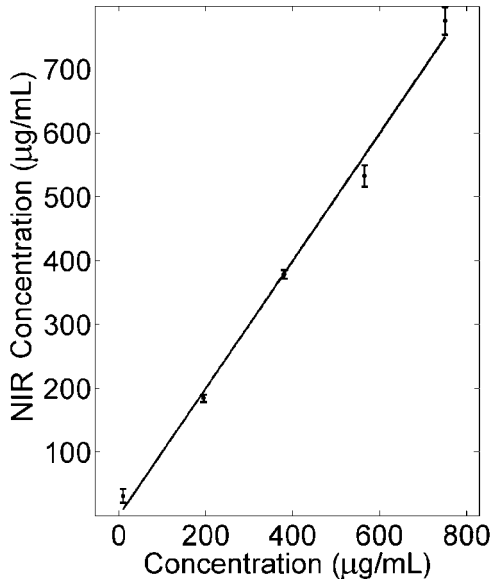

Fig. 4. NIR calibration line for estradiol in ethanol using net analyte signal for the prediction of solution concentrations, $r^2 = 0.988$, SEE = 3.46%, SEP = 4.01%.

analytical method (usually the same method employed to provide reference values for the calibration samples).

NAS calibration offers a distinct advantage over these methods, namely the potential for one-point calibration. When the experimenter has a set of pure component spectra for each of the system components, and a matrix of spectra without the analyte, it is a simple matter to identify the portion of the signal orthogonal to the interferences. If the NAS is the portion of the signal the experimenter is looking for, it will correlate highly to a change in concentration of the analyte of interest. If it is not the right signal, it will not correlate to the desired change in concentration. Therefore, NAS accomplishes with one-point calibration what other chemometric models require an entire calibration set to accomplish. This offers a distinct advantage in time and in the computational burden for analysis of NIR spectra.

It was important to confirm the versatility and sensitivity of this NIR method in human tissue, as some species differences in the biochemical make-up of the skin exist, and the barrier properties of human skin are also more resistant as compared to rodent skin. In our previous *in vitro* study (7) with guinea pig skin, the skin contents of EN were found to be generally higher than with the human skin studied here. For example, a statistically significant ($p < 0.05$) 14-fold difference between the EN content in the human skin (103 ± 21 μg/g) and the guinea pig skin [1497 ± 345 μg/g, (7)] after a 15 h exposure to the saturated EN solution was observed (Student's t-test, SigmaStat, SPSS, Inc., Chicago, IL). For topical and transdermal studies, hairless guinea pig skin is a close approximation of human skin. Skin permeability studies with many compounds indicate that hairless guinea pig skin is more similar to human skin than either rat skin or hairless mice skin (20,21). However, some morphological and biochemical differences do exist between the two, as the stratum corneum in the hairless guinea pig is composed of only a few layers (22). The increased permeability of drugs through guinea pig skin, as compared to human skin, is most likely due to the lack of the multilayered stratified and resistant stratum corneum structure. Other studies have shown that there are also some immune and biochemical differences between guinea pig and human skin (23). Each of these differences contributed to the decreased drug permeation in the human tissue as compared to the previously-studied guinea pig skin. Additionally, light scatter was noticeably more pronounced in human tissue, as is evident from Fig. 7. A NIR scan of human tissue and guinea pig

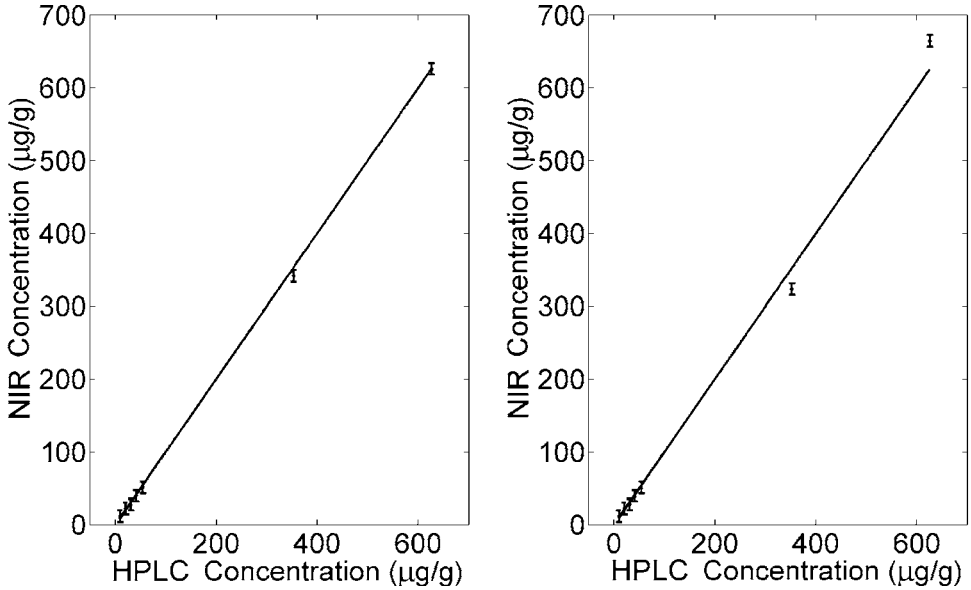

Fig. 5. NIR calibration line from human skin treated with an applied dose of estradiol in ethanol, (*left*) epidermis calibration, $r^2 = 0.987$, SEE = 3.30%, SEP = 5.66%, (*right*) dermis calibration, $r^2 = 0.967$, SEE = 5.53%, SEP = 6.83%. The *diagonal line* illustrates the perfect correlation between HPLC and NIR, HPLC concentrations are shown on the *x-axis*, and the *error bars* are the means and standard errors of the NIR measurements.

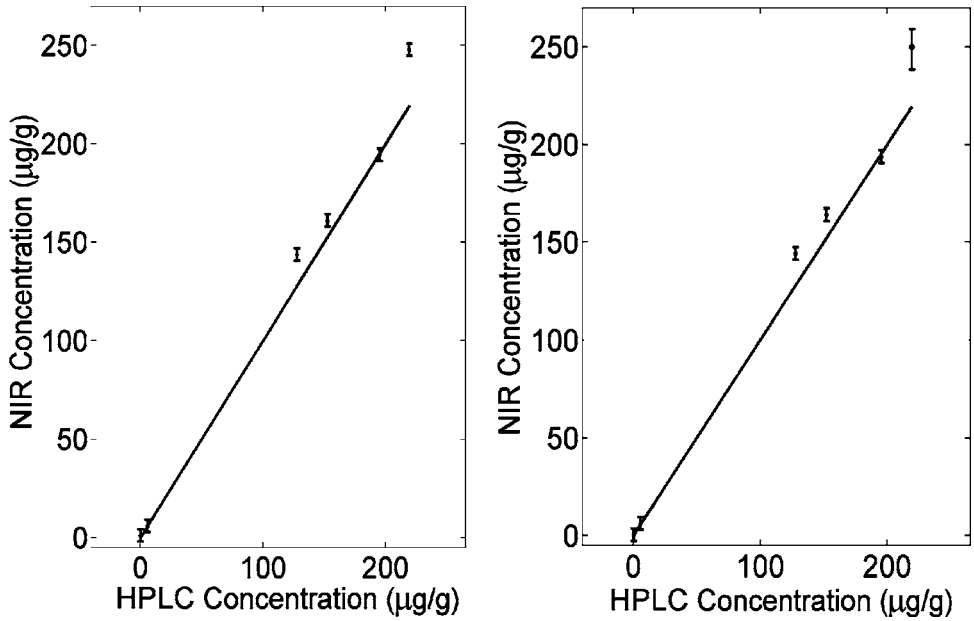

Fig. 6. NIR calibration line from human skin treated with an applied dose of either 50 mg of placebo cream or 1% econazole nitrate cream, (*left*) dermis calibration, $r^2 = 0.981$, SEE = 5.67%, SEP = 6.07%, (*right*) epidermis calibration, $r^2 = 0.980$, SEE = 5.93%, SEP = 6.71%. The outlier is not included in this model.

tissue treated with drug vehicle demonstrates that while the spectral features are similar between the two models, the absolute signal was far smaller in human tissue. This did not, however, affect the predictive ability of the NIR.

Great Flexibility and Durability

This experiment applied NIR spectroscopic analysis in four different applications; drug powders, drug in solution, and tissue concentrations of drug after exposure to solutions and creams. Additionally, it successfully measured drug concentrations in both guinea pig skin and human skin. The strong correlation of NIR concentration prediction to the HPLC results suggests that NIR spectrometry is a flexible technique for analysis of tissue concentrations of drugs and other chemicals after topical exposure. Once the method was established, no NIR spectra had to be discarded from a sample set consisting of 44 tissue samples and 264 scans, suggesting that NIR is a very reliable method of analysis. For the duration of this experiment, there were no failures or erroneous spectra. When the NIR does fail, a short noise spike from the preamplifier causes a very distinct and easily identifiable spectral feature, making it a simple matter to locate and discard.

NIR is also a nondestructive and rapid method of analysis, taking less than 2 min to complete each scan. In this research, samples were simply placed on a microscope slide and scanned, thus no sample preparation is required. NIR also has the capability of being a noninvasive method of analysis. Using a fiber-optic probe it is possible to scan skin tissue *in vivo* in whole animal or clinical studies. Skin samples in this research were scanned inside a closed metal chamber, thus external light and room noise were not a factor. In the chamber, NIR spectra are essentially free from external noise and interference. The limit of detection can be approximated as the concentration at which the S/N ratio is equal to three (13). The lowest drug concentrations measured in this research were 11.5 µg/g for EST and 26.4 µg/g for EN, and in both cases the S/N ratios were greater than three. The NIR dynamic range can be expressed as the region of the NIR that responds linearly to a change in concentration. Since this experiment did not exceed the upper or lower limits of detection, the dynamic range is simply the range of concentrations used. For EST, the dynamic range was 0–625.4 µg/g, and for EN the dynamic range was 0–125.8 µg/g. These results demonstrate that EN and EST can be measured in human skin at clinically relevant detection levels, because we have applied clinically relevant doses of EN cream and EST solution in the diffusion studies.

CONCLUSION

NIR spectrometry in combination with a NAS multivariate regression demonstrated the ability to measure dermal

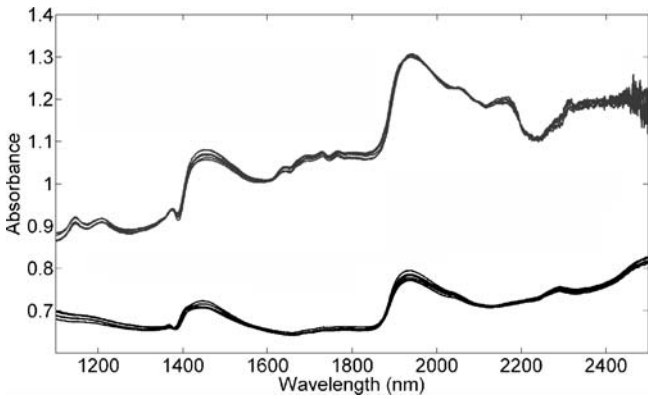

Fig. 7. Raw NIR spectra from guinea pig skin (*top*) and human skin (*bottom*) treated with drug vehicle only (propylene glycol).

absorption from estradiol in ethanol, econazole nitrate in propylene glycol, and a 1% econazole nitrate cream in human tissue samples with a very high degree of success. This suggests that NIR could serve as a noninvasive, rapid, and accurate alternative to the other topical bioavailability/bioequivalence analytical methods in use today.

ACKNOWLEDGMENT

This research was sponsored by the Food and Drug Administration, contract number D3 922004.

REFERENCES

1. L. K. Pershing, J. L. Nelson, J. L. Corlett, S. P. Shrivastava, D. B. Hare, and V. Shah. Assessment of dermatopharmacokinetic approach in the bioequivalence determination of topical tretinoin gel products. *J. Am. Acad. Dermatol.* **48**(5):740–751 (2003).
2. M. Kreilgaard, M. B. Kemme, J. Burggraaf, R. C. Schoemaker, and A. F. Cohen. Influence of a microemulsion vehicle on cutaneous bioequivalence of a lipophilic model drug assessed by microdialysis and pharmacodynamics. *Pharm. Res.* **18**(5):593–599 (2001).
3. D. Wierenga and C. R. Eaton. Phases of product development—drug development and approval process. Alliance Pharmaceutical Corporation. Retrieved March 23, 2006. <http://www.allp.com/drug_dev.htm>.
4. F. Pirot, Y. N. Kalia, A. L. Stinchcomb, G. Keating, A. Bung, and R. H. Guy. Characterization of the permeability barrier of human skin *in vivo*. *Proc. Natl. Acad. Sci. USA* **94**:1562–1567 (1997).
5. A. L. Stinchcomb, F. Pirot, G. D. Touraille, A. L. Bunge, and R. H. Guy. Chemical uptake into human stratum corneum *in vivo* from volatile and non-volatile solvents. *Pharm. Res.* **16**(8):1288–1293 (1999).
6. M. B. Reddy, A. L. Stinchcomb, R. H. Guy, and A. L. Bunge. Determining dermal absorption parameters *in vivo* from tape strip data. *Pharm. Res.* **19**(3): 292–298 (2002).
7. J. Medendorp, J. Yedluri, D. C. Hammell, T. Ji, R. A. Lodder, and A. L. Stinchcomb. Near infrared spectrometry for the quantification of dermal absorption of econazole nitrate and 4-cyanophenol. *Pharm. Res.* **23**(4):835–843 (2006).
8. A. Urbas, M. W. Manning, A. Daugherty, L. A. Cassis, and R. A. Lodder. Near-infrared spectrometry of abdominal aortic aneurysm in the ApoE−/− mouse. *Anal. Chem.* **75**:3650–3655 (2003).
9. B. Dai, A. Urbas, and R. A. Lodder. Sensor batteries: implantable sensor batteries. *NIR News* **17**(1):14–15 (2006).
10. Introduction to NIR technology. Analytical Spectral Devices, Inc. Retrieved February 12, 2006. http://www.asdi.com/ASD-600510_NIR-Introduction.pdf.
11. H. M. Boelens, W. T Kok, O. E. Noord, and A. K. Smilde. Performance optimization of spectroscopic process analyzers. *Anal. Chem.* **76**:2656–2663 (2004).
12. A. Lorber. Error propagation and figures of merit for quantification by solving matrix equations. *Anal. Chem.* **58**:1167–1172 (1988).
13. K. S. Booksh, and B. R. Kowalski. Theory of analytical chemistry. *Anal. Chem.* **66**(15):782a–791a (1994).
14. A. Lorber, K. Faber, and B. R. Kowalski. Net analyte signal calculation in multivariate calibration. *Anal. Chem.* **69**(8):1620–1626 (1997).
15. W. Fountain, K. Dumstorf, A. E. Lowell, R. A. Lodder, and R. J. Mumper. Near-infrared spectroscopy for the determination of testosterone in thin-film composites. *J. Pharm. Biomed. Anal.* **33**(2)1:181–189 (2003).
16. R. A. Lodder, M. Selby, and G. Hieftje. Detection of capsule tampering by near-infrared reflectance analysis. *Anal. Chem.* **59**:1921–1930 (1987).
17. I. T. Jolliffe. *Principal Component Analysis*, Springer, Berlin Heidelberg New York, 2002.
18. R. Leardi and L. Norgaard. Sequential application of backward interval partial least squares and genetic algorithms for the selection of relevant spectra regions. *J. Chemom.* **18**:486–497 (2004).
19. O. E. Noord. Elimination of uninformative variables for multivariate calibration. *Anal. Chem.* **68**:3851–3858 (1996).
20. K. C. Moon, R. C. Wester, and H. I. Maibach. Diseased skin models in the hairless guinea pig skin: *in vivo* percutaneous absorption. *Dermatologica* **180**:8–12 (1999).
21. R. Panchagnula, K. Stemmer, and W. A. Ritschel. Animal models for transdermal drug delivery. *Methods Find. Exp. Clin. Pharmacol.* **19**:335–341 (1997).
22. L. L. Ferry, G. Argentieri, and D. H. Lochner. The comparative histology of porcine and guinea pig skin with respect to iontophoretic drug delivery. *Pharm. Acta Helv.* **70**:43–56 (1995).
23. X. Jia, Z. Zhu, and C. Li. Immune and biochemical analysis of protein of homogenates of three different kinds of skin. *Zhonghua Zheng Xing Shao Shang Waike Za Zhi* **12**(1):51–53 (1996).